*Cerebral Cortex*, February 2018;28: 433–446

**doi: 10.1093/cercor/bhw377**
Advance Access Publication Date: 20 December 2016
Original Article

ORIGINAL ARTICLE

# Early Alterations of Hippocampal Neuronal Firing Induced by Abeta42

Daniela Gavello[1], Chiara Calorio[1], Claudio Franchino[1], Federico Cesano[2], Valentina Carabelli[1], Emilio Carbone[1], and Andrea Marcantoni[1]

[1]Department of Drug Science and Technology, Torino University, Corso Raffaello 30, 10125 Torino, Italy and [2]Department of Chemistry Via Pietro Giuria 7, Torino University, 10125 Torino, Italy

Address correspondence to Andrea Marcantoni. Department of Drug Science and Technology, Torino University, Corso Raffaello 30, 10125 Torino, Italy. Email: andrea.macantoni@unito.it



## Abstract

We studied the effect of Amyloid β 1-42 oligomers (Abeta42) on $Ca^{2+}$ dependent excitability profile of hippocampal neurons. Abeta42 is one of the Amyloid beta peptides produced by the proteolytic processing of the amyloid precursor protein and participates in the initiating event triggering the progressive dismantling of synapses and neuronal circuits. Our experiments on cultured hippocampal network reveal that Abeta42 increases intracellular $Ca^{2+}$ concentration by 46% and inhibits firing discharge by 19%. More precisely, Abeta42 differently regulates ryanodine (RyRs), NMDA receptors (NMDARs), and voltage gated calcium channels (VGCCs) by increasing $Ca^{2+}$ release through RyRs and inhibiting $Ca^{2+}$ influx through NMDARs and VGCCs. The overall increased intracellular $Ca^{2+}$ concentration causes stimulation of $K^+$ current carried by big conductance $Ca^{2+}$ activated potassium (BK) channels and hippocampal network firing inhibition. We conclude that Abeta42 alters neuronal function by means of at least 4 main targets: RyRs, NMDARs, VGCCs, and BK channels. The development of selective modulators of these channels may in turn be useful for developing effective therapies that could enhance the quality of life of AD patients during the early onset of the pathology.

**Key words:** big conductance $Ca^{2+}$ activated potassium (BK) channels, NMDA receptors, ryanodine receptors, spontaneous calcium transients, voltage gated $Ca^{2+}$ channels

## Introduction

Among the various hallmarks of Alzheimer's disease (AD), the activation process of the "amyloid-cascade" is one of the most studied. It assumes that the accumulation of oligomers of Amyloid Beta peptides (Abeta), produced by the proteolytic processing of the amyloid precursor protein (APP) is the initiating event that triggers the progressive dismantling of synapses, neuronal circuits, and networks (Palop and Mucke 2010). However, so far there are not yet clear data regarding any possible Abeta-induced impairment of neuronal network excitability. Our previous results indicate that in Tg2576 mice neurons from lateral entorhinal cortex (LEC) (Marcantoni et al. 2014) are characterized by early impairments of their excitable profile. Tg2576 mice harbor the human APP gene with the Swedish mutation and display age-dependent accumulation of Abeta peptides, like Abeta40, Abeta42, Abeta*56, and exhibit hyperphosphorylated tau (Hsiao et al. 1996). The use of these mice does not therefore clarify if one or more Abeta peptides cause neuronal dysfunctions. These latter are generated by multiple interactions between Abeta oligomers and neurons that could occur by their direct binding to membrane receptors, interaction with membrane lipids leading to pore channels formation or changes of membrane properties (Benilova et al. 2012). The manifold mechanisms of interplay between Abeta peptides and neurons are followed by variable effects on neurons and vary from synaptic plasticity impairment (Puzzo et al. 2015) to spines and cells loss. Here, we propose to focus on the effects of Amyloid β 1–42 oligomer (Abeta42), whose accumulation induces early and severe neuronal function impairments

(Lambert et al. 1998; Ripoli et al. 2013). There are however contrasting findings concerning the effect of Abeta42 on neuronal excitability and synaptic function. Recent evidences show that spontaneous firing of cultured neuronal network recorded by means of microelectrode arrays (MEAs) is depressed by Abeta42 (Charkhkar et al. 2015), that in turn inhibits synaptic function (Ripoli et al. 2013). Other evidences indicate that Abeta42 enhances neuronal excitability (Minkeviciene et al. 2009; Puzzo et al. 2009; Tamagnini et al. 2015). All together these results suggest that the effect of Abeta42 strongly depends on its concentration and aggregation state (Palop and Mucke 2010), but they fail to clarify its mechanism of action. Likewise, the existence of a correlation between excitatory impairments and $Ca^{2+}$ dysregulation induced by Abeta42 is still not completely understood. $Ca^{2+}$ regulates many neuronal functions such as gene transcription, excitability, and synaptic activity. It is generally accepted that during AD both the mechanisms of $Ca^{2+}$ entry (Thibault et al. 2012; Wang and Mattson 2013) and $Ca^{2+}$ release (Stutzmann et al. 2004; Oules et al. 2012) are altered. This is shown both in transgenic mice (Oules et al. 2012; Chakroborty et al. 2013) and in neurons treated with Abeta peptides (Mattson 2010) as well as Abeta42 (Lazzari et al. 2014). Here, we studied the effect of Abeta42 on the $Ca^{2+}$ dependent excitatory profile of hippocampal neurons using MEAs extracellular recordings on neuronal circuits, intracellular patch clamp recordings, and $Ca^{2+}$ fluorescence imaging on single neurons. When maintained in primary culture, hippocampal neurons generate spontaneous bursts of action potentials (Gavello et al. 2012; Allio et al. 2015) that occur in synchrony with phasic periods of $Ca^{2+}$ entry (Murphy et al. 1992). These neurons are in fact connected by synaptic contacts morphologically and physiologically similar to those present in vivo and are useful to investigate the relationship between excitability and synaptic function. We found that pre-incubation of neurons with Abeta42 raises intracellular $Ca^{2+}$ concentration and causes a paradoxical firing inhibition. We suggest that Abeta42 stimulates $Ca^{2+}$ to be released through ryanodine receptors (RyRs) and inhibits $Ca^{2+}$ influx through NMDA receptors (NMDARs) as well as through voltage gated calcium channels (VGCCs). The Abeta42-induced $Ca^{2+}$ release activates presynaptic BK $Ca^{2+}$ activated potassium channels and inhibits neuronal firing by mainly acting at presynaptic glutamatergic terminals.

## Material and Methods

### Abeta42 Preparation

Abeta42 (Sigma-Aldrich) was dissolved in 1% ammonium hydroxide solution and stored at −20 °C at a concentration of 1 mM. Before neuronal administration Abeta42 was dissolved into the culture medium at the experimental concentration of 1 μM. For the aggregation protocol the peptide was stored 24 h at 4 °C to obtain oligomers and 48 h at room temperature before incubation with neurons (Dahlgren et al. 2002; Tamagno et al. 2006). Unless indicated otherwise, the results were always obtained by comparing control neurons treated with picrotoxin (100 μM) for 48 h versus neurons incubated for 48 h with Abeta42 together with picrotoxin.

### AFM (Atomic Force Microscopy)

Measurements were performed in the intermittent-contact regime (tapping-mode AFM, pyramidal cantilever with a tip radius <6 nm) by using a modified Nanosurf Easyscan2 AFM instrument, equipped with a 10 μm high-resolution scan head, shielded by an acoustically insulated enclosure and placed on an anti-vibration platform. Before analysis, sample solution containing Abeta42 oligomers or fibrils at a concentration of 1 μM were diluted to 100 nM and then dropped on freshly cleaved mica. Samples were AFM imaged as soon as supports become dry.

### Cell Culture

All experiments were performed in accordance with the guidelines established by the National Council on Animal Care and approved by the local Animal Care Committee of Turin University. Hippocampal neurons were obtained from c57bl6 mouse 18-day embryos. Hippocampus was rapidly dissected under sterile conditions, kept in cold HBSS (4 °C) with high glucose, and then digested with papain (0.5 mg/mL) dissolved in HBSS plus DNAse (0.1 mg/mL) as previously described (Gavello et al. 2012). Isolated cells were then plated at the final density of 1200 cells/$mm^2$ onto the MEA (previously coated with poly-DL-lysine and laminine). Cells were incubated with 1% penicillin/streptomycin, 1% glutamax, 2.5% fetal bovine serum, 2% B-27 supplemented neurobasal medium in a humidified 5% $CO_2$ atmosphere at 37 °C. Each MEA dish was covered with a fluorinated ethylene–propylene membrane (ALA scientific) to reduce medium evaporation and maintain sterility, thus allowing repeated recordings from the same chip. Recordings were carried out at DIV 18.

### Patch Clamp Experiments

Patch electrodes, fabricated from thick borosilicate glasses (Hilgenberg), were pulled to a final resistance of 3–5 MΩ. Patch clamp recordings were performed in whole cell configuration using a Multiclamp 700-B amplifier connected to a Digidata 1440 and governed by the pClamp10 software (Axon Instruments, Molecular Devices Ltd).

Experiments were performed at room temperature (22–24 °C) in whole cell configuration and acquired with sample frequency of 10 KHz (Baldelli et al. 2002, 2005). Analysis was performed with Clampfit software (Axon Instruments). Data are expressed as means ± SEM and statistical significance was calculated by using Student's *t*-test. Values of $P < 0.05$ were considered significant. Where indicated, analysis of variance (ANOVA) followed by Bonferroni post hoc test was used and *P*-values <0.05 were considered significant.

### Current Clamp

Neurons were clamped at −70 mV ($V_h$) and depolarized for 50 ms by injecting 800 pA of current.

### Voltage Clamp

For $Ca^{2+}$ current recording neurons were hold at −70 mV ($V_h$) and depolarized for 50 ms at −10 mV in order to maximally activate inward $Ca^{2+}$ current. $K^+$ currents were recorded by depolarizing neurons from −70 to +80 mV for 400 ms. Where indicated the depolarizing step was preceded by stimuli of increased duration (from 10 to 90 ms) to −10 mV to open all available VGCCs (Marcantoni et al. 2010). AMPA dependent eEPSCs following spontaneous action potential (APs) or electrical stimulation were recorded by holding neurons at −70 mV ($V_h$). Presynaptic electrical stimuli were delivered through a glass pipette (1 μm tip diameter) filled with Tyrode's solution and placed in contact with the soma of presynaptic neuron in a loose-seal configuration. eEPSCs were filtered at half the acquisition rate with 8-pole low-pass Bessel filter. Recording with leak current >100 pA or series resistance >20 MΩ was discarded. Current pulses of 0.1 ms and variable

amplitude (10–45 μA) were generated by an isolated pulse stimulator (model 2100; A-M Systems, Carlsburg).

### MEA Recordings

Multisite extracellular recordings from 60 electrodes were performed using the MEA-system, purchased from Multi-Channel Systems. Data acquisition were controlled through MC_Rack software (Multi-Channel Systems), setting the threshold for spike detection at −30 μV and sampling at 10 kHz. Experiments were performed in a non-humidified incubator at 37 °C and with 5% $CO_2$, without replacing the culture medium. Before starting the experiments, cells were allowed to stabilize in the non-humified incubator for 90 s; then the spontaneous activity was recorded for 2 min.

Culture medium was supplemented with picrotoxin (100 μM, Sigma-Aldrich) for inhibiting the GABAergic synaptic currents.

### Analysis of MEA Activity

Bursts analysis was performed using Neuroexplorer software (Nex Technologies) after spike sorting operations. A burst consists of a group of spikes with decreasing amplitude, thus we set a threshold of at least 3 spikes and a minimum burst duration of 10 ms. We set interval algorithm specifications such as maximum interval to start burst (0.17 s) and maximum interval to end burst (0.3 s) recorded in 0.02 s bins (Gavello et al. 2012). Burst analysis was performed by monitoring the following parameters: mean frequency, number of bursts, and mean burst duration. Cross correlation probability values were obtained by means of Neuroexplorer software using ±2 s and 5 ms bin size.

Data are expressed as means ± SEM and statistical significance was calculated by using Student's *t*-test. Values of $P < 0.05$ were considered significant. The number of experiments is referred to the number of MEA each of those consisted of 59 recording electrodes.

### Calcium Imaging

Hippocampal neurons plated on glass petri dishes were loaded with the fluorescent $Ca^{2+}$ indicator Fura2-AM dye (3 μM) (Invitrogen, Molecular Probes) for 1 h. The fluorescent dye was then washed, and extracellular solution containing picrotoxin (100 μM) was replaced into the petri dish. The inverted microscope used (Leica DMI3000B) was equipped with a short-arc xenon gas discharge lamp (Ushio, Cypress). Alternating excitation wavelengths of 340 and 380 nm were obtained by a monochromator (Till Photonics). The emitted fluorescence was measured at 500–530 nm. Images were projected onto a EMCCD camera (QuantEM:512SC, Photometrics) and stored every 200 ms. Spontaneous $Ca^{2+}$ transients were recorded both in control condition and after incubation with Abeta42 using Metafluor software (Molecular Devices) for data acquisition. The relative change in fluorescence (ΔF/F) was measured considering the peak of $Ca^{2+}$ transients. Data are expressed as means ± SEM and statistical significance was calculated by using Student's *t*-test. Values of $P < 0.05$ were considered significant.

### Solutions and Drugs

For voltage clamp recording of $Ca^{2+}$ currents the external solution contained (in mM): 135 TEACl, 2 $CaCl_2$, 2 $MgCl_2$, 10 HEPES, 10 glucose (pH 7.4 with CsCl). The internal solution contained (in mM): 90 CsCl, 20 TEACl, 10 EGTA, 10 Glucose, 1 MgCl, 4 ATP, 0.5 GTP, 15 Phosphocreatine (pH 7.4 with CsOH). For $Ca^{2+}$ current recording, 300 nM TTX (Tocris Bioscience), 1 mM kynurenic acid (Sigma-Aldrich), 100-μM picrotoxin were added to extracellular solution.

When $K^+$ current recording, Tyrode's Standard solution was used as extracellular solution and the intracellular solution was the same used in current clamp experiments.

For current-clamp recording extracellular Tyrode's Standard solution contained (in mM) 2 $CaCl_2$, 130 NaCl, 2 $MgCl_2$, 10 Hepes, 10 glucose, 4 KCl (pH 7.4). The intracellular solution contained (in mM): 135 gluconic acid (potassium salt: K-gluconate), 5 NaCl, 2 MgCl2, 10 HEPES, 0.5 EGTA, 2 ATP-Tris, 0.4 Tris-GTP.

Nifedipine and paxilline were used to block, respectively, L-type $Ca^{2+}$ channels (LTCCs) and BK channels (Marcantoni et al. 2010) while apamine (200 nM) was used to inhibit SK channels (Vandael et al. 2012). All these compounds were purchased from Sigma-Aldrich.

eEPSCs were recorded by perfusing postsynaptic neurons with Tyrode's Standard solution supplemented with D-(-)-2-amino-5-phosphonopentanoic acid (D-AP5; 50 μM), picrotoxin (100 μM), and CGP58845 (5 μM) (Tocris) to avoid contamination from NMDA dependent and GABAergic receptors activated currents. Action potential driven eEPSCs were recorded by adding Tetrodoxin (10 nM) to limit polysynaptic activity (Raffaelli et al. 2004). The standard internal solution was (in mM): 20 Cs-$MSO_3$, 90 CsCl, 10 Hepes, 5 EGTA, 2 $MgCl_2$, 4 ATP (disodium salt), 15 Phosphocreatine (pH 7.4). Electrically stimulated eEPSCs were recorded by adding QX-314 (N-(2,6-dimethylphenyl carbamoylmethyl) triethylammonium bromide; 10 mM; Tocris) into the internal solution to block postsynaptic $Na^+$ currents.

For $Ca^{2+}$ imaging experiments the extracellular solution contained (in mM): 130 NaCl, 4 KCl, 2 $CaCl_2$, 10 Glucose, 10 Hepes, 0.8 $MgCl_2$, 0.4 Glicine (pH 7.4).

Where indicated, 6,7-Dinitroquinoxalone-2,3-Dione (DNQX, 20 μM, Sigma-Aldrich) and dantrolene (10 μM, Sigma-Aldrich) were used for blocking, respectively, AMPA dependent synaptic currents and RyRs.

## Results

### Role of Somatic Action Potential and Neurotransmitter Release in Governing Spontaneous Firing of Hippocampal Network

As already observed (Bacci et al. 1999; Arnold et al. 2004; Gavello et al. 2012) after 18 days in vitro (DIV), networks of cultured hippocampal neurons fire spontaneously (Fig. 1*a*). TTX-sensitive $Na^+$ channels are critical for somatic AP generation and their block by 0.3 μM TTX caused the complete inhibition of spontaneous firing (Fig. 1*a*, top). Glutamatergic synapses are crucial as well for governing spontaneous depolarizations (Arnold et al. 2004). In particular the block of glutamate release through the administration of the selective P/Q $Ca^{2+}$ channels blocker ω-Agatoxin IV A (Fig. 1*a*, middle) completely inhibited spontaneous firing by preventing $Ca^{2+}$ dependent neurotransmitter release. The selective blocker of glutamatergic AMPA receptors (AMPARs) DNQX (20 μM) completely abolished hippocampal electrical activity as well (Fig. 1*a*, bottom). As previously observed (Arnold et al. 2004), 1 h after the block of GABAA receptors with picrotoxin (100 μM), the firing frequency of control neurons increased from 0.9 ± 0.1 Hz to 2.5 ± 0.2 Hz ($n = 9$, $^{***}P < 0.001$) and tend to decrease over time (Fig. 1*b*,*c*). We focused on the effect of picrotoxin after 48–72 h from its incubation observing the generation of more regular and synchronized bursts of APs (Fig. 1*c* white vs. gray panels). All together these results indicate that spontaneous

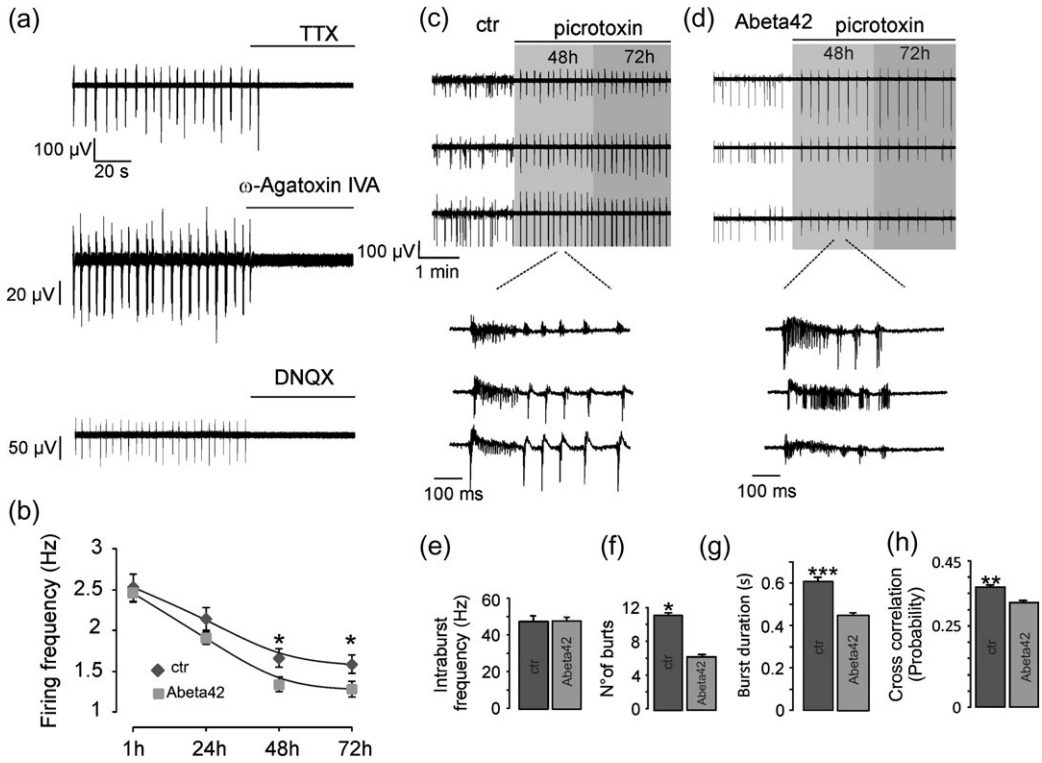


**Figure 1.** (*a*) Spontaneous hippocampal electrical activity measured by means of MEAs by one representative recording channel at 18 DIV after 1 h of incubation with picrotoxin. *top*) Spontaneous hippocampal electrical activity depends on the availability of TTX-sensitive somatic Nav1 channels. *middle*) The block of glutamate release through administration of presynaptic Cav 2.1 channels blocker ω-Agatoxin IVA (2 μM) completely inhibits spontaneous firing by preventing $Ca^{2+}$ dependent neurotransmitter release. *bottom*) The selective AMPARs inhibitor DNQX completely abolishes hippocampal electrical activity (*b*) Time course of hippocampal network firing frequency recorded from 1 to 72 h after incubation with picrotoxin alone (control, dark gray diamonds) and together with Abeta42 (1 μM) (light gray squares). After 48 and 72 h of incubation with picrotoxin the firing frequency is significantly decreased by Abeta42. (*c*) Selection of 3 representative recording traces from the same MEA showing neuronal spontaneous firing in control conditions at 18 DIV (white) and after exposure to picrotoxin (100 μM) for respectively 48 (light gray panel) and 72 h (dark gray panel). The 2 insets refer to the magnification of single bursts of action potentials. (*d*) Three representative recording traces from the same MEA showing the inhibition of spontaneous firing by Abeta42 (1 μM). Neuronal firing was recorded at 18 DIV before administration of Abeta42 and picrotoxin (white panel) and compared with that measured after 48 h (light gray panel) and 72 h (dark gray panel) from administration of Abeta42 together with picrotoxin. After 48 h (light gray bar) the intraburst firing frequency remains unaffected (*e*) while both number of bursts (*f*), bursts duration (*g*), and cross correlation (*h*) decrease significantly with respect to controls (dark gray bar).

network depolarizations depend on both somatic APs and neurotransmitter release that mainly involves postsynaptic AMPA and GABAergic receptors.

## Abeta42 Oligomers Inhibit Spontaneous Firing of Hippocampal Network

Although it is already known that amyloid beta peptides impair glutamatergic synaptic functions (Palop and Mucke 2010), here we focused on the effects of Abeta42 on spontaneous firing mediated by the activation of excitatory synapses. We therefore incubated neurons with Abeta42 (1 μM) together with picrotoxin (Fig. 1*d*) and measured the firing activity after 1–72 h. Similarly to what observed in control neurons, after 1 h of incubation with Abeta42 together with picrotoxin, firing frequency increased from 1.2 ± 0.1 Hz to 2.4 ± 0.1 Hz ($n = 11$, $^{***}P < 0.001$) (Fig. 1*b*), but after 48 and 72 h (Fig. 1*d*, gray panels) it was significantly reduced by Abeta42 if compared to what observed in control neurons ($^{*}P < 0.05$). In particular, after 48 h of incubation with Abeta42 and picrotoxin the firing frequency was on average 1.3 ± 0.1 Hz ($n = 11$) while control neurons displayed an average firing frequency of 1.6 ± 0.1 Hz ($n = 9$). Further analysis revealed that after 48 h of incubation with Abeta42 the intraburst firing frequency remained unaffected (Fig. 1*e*), while the number of bursts (Fig. 1*f*), bursts duration (Fig. 1*g*), and the cross correlation values (Fig. 1*h*) decreased significantly. All together these results suggest that Abeta42 decreases the firing activity in mature hippocampal network. We tested the possibility that the effect of Abeta42 oligomers depended on their concentration (Puzzo et al. 2009; Lee et al. 2013). We therefore reduced the concentration of Abeta42 to 200 nM and after 48 h of incubation we observed again a firing frequency inhibition from 1.6 ± 0.1 Hz ($n = 6$) to 1.0 ± 0.1 Hz ($n = 9$, $^{***}P < 0.001$, not shown). In order to understand if the effect of Abeta42 depended by its aggregation state (Lambert et al. 1998; Dahlgren et al. 2002), we further treated hippocampal neurons with Abeta42 previously stored for 48 h at 37 °C (Dahlgren et al. 2002). Following this procedure we observed, through AFM, that Abeta42 (1 μM) assembled in fibrils of 1–2 μM length 5–14 nM thickness (see Supplementary Fig. 1). MEA recordings showed that incubation with Abeta42 fibrils for 48 h did not inhibit firing frequency that was 2.2 ± 0.4 Hz ($n = 5$) in control and 2.6 ± 0.2 Hz ($n = 4$) in neurons incubated with Abeta42 fibrils, $P = 0.4$) (not shown). We thus confirmed that Abeta42 dependent firing inhibition is influenced by its aggregation state and is detectable during the early phase of its production, when Abeta42 form oligomers rather than fibrils (Palop and Mucke 2010). From here on we thus performed experiments using Abeta42 only in the oligomeric form as described in the methods section at a

concentration of 1 μM. Under these conditions AFM microscopy revealed that Abeta42 oligomers were characterized by a globular shape of average diameter of 10–100 nm and height comprised between 2 and 4 nm (Supplementary Fig. 1), in line with what recently proposed by others (Manassero et al. 2016).

## Abeta42 Oligomers Increase the Amplitude of Spontaneous $Ca^{2+}$ Transients by Potentiating $Ca^{2+}$ Released from RyRs

Spontaneous intracellular $Ca^{2+}$ oscillations occur regularly in primary cultured hippocampal neurons (Fig. 2*a*). Abeta42 increased their amplitude by 46%, without affecting their frequency and the basal intracellular $Ca^{2+}$ concentration (Fig. 2*b*). Average ΔF/F values increased from 1.26 ± 0.11 ($n$ = 39) in control neurons to 1.84 ± 0.23 ($n$ = 30) in neurons incubated with Abeta42 for 48 h (Fig. 2c, *P < 0.05). Being postulated the ability of Abeta42 to form $Ca^{2+}$ permeable pores in the plasma membrane (Demuro et al. 2011), we measured whether changes in membrane resistance ($R_m$) were detectable after incubation of neurons with Abeta42. To this purpose, we performed patch-clamp recordings by holding neurons at −70 mV and injecting 50 pA negative current (not shown). The degree of hyperpolarization was measured and the correspondent value of $R_m$ calculated in control neurons (0.19 ± 0.03 GΩ, $n$ = 16) was comparable with that obtained in the presence of Abeta42 (0.18 ± 0.04, $n$ = 7). The $Ca^{2+}$ transients are generated by $Ca^{2+}$ influx through plasma membrane and $Ca^{2+}$ released from intracellular stores when $IP_3$ and/or RyRs are activated. Considering the relevance of RyRs in AD onset and progression (Oules et al. 2012; Chakroborty et al. 2013), we analyzed their contribution in the generation of spontaneous $Ca^{2+}$ transients. As already observed in chick motoneurons (Wang et al. 2009) here we found that in control neurons RyRs contribute to the generation of spontaneous $Ca^{2+}$ transients (Fig. 2*d*), but they are scarcely involved in the regulation of firing activity (Cheong et al. 2011) (Fig. 2*e*). The selective RyRs negative allosteric modulator dantrolene (10 μM) reduced indeed the peak amplitude of spontaneous $Ca^{2+}$ transients by 31.9 ± 8.7% ($n$ = 8) (Fig. 2*f*) without altering the firing frequency (Fig. 2*g*) and increasing by 17.0 ± 7.7% the cross correlation (Fig. 2*h*). Dantrolene mediated inhibition of $Ca^{2+}$ transients in neurons treated with Abeta42 for 48 h (Fig. 2*i*,*f*) was significantly larger than in control conditions (54.0 ± 5.6%, $n$ = 8, *P < 0.05), while the firing frequency (Fig. 2*l*,*g*) and the cross correlation (Fig. 2*h*) values increased, respectively, by 13.3 ± 5.5% ($n$ = 9) and 53.6 ± 14.8% (***P < 0.001) after

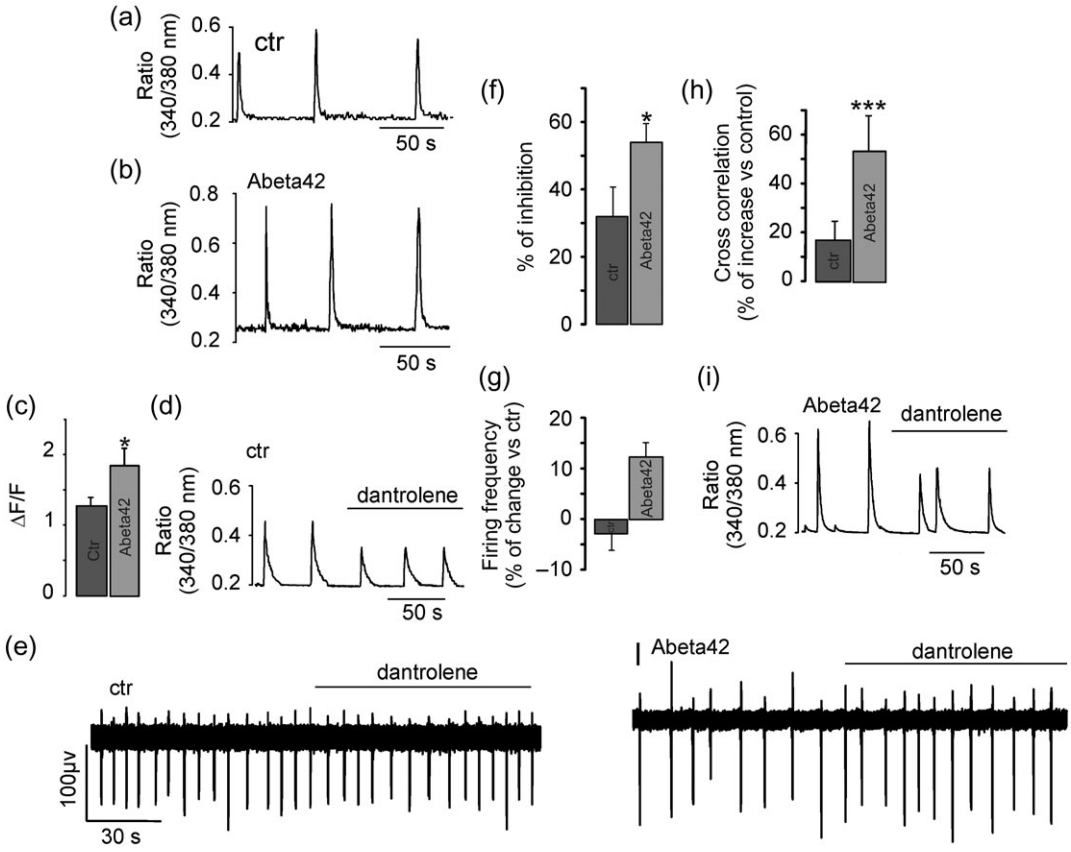


**Figure 2.** (*a*) After 18 DIV hippocampal network generates spontaneous $Ca^{2+}$ transients whose amplitude is significantly increased (*b*) after incubation for 48 h with Abeta42. (*c*) Bar graph summarizing the increased amplitude of $Ca^{2+}$ transients induced Abeta42 (light gray bar) with respect to controls (dark gray bars). (*d*) In control conditions, the inhibition of RyRs with dantrolene decreases the amplitude of $Ca^{2+}$ transients. (*e*) MEA recording showing that in control neurons spontaneous firing is not influenced by dantrolene. (*f*) Bar graph comparing the more pronounced inhibition of $Ca^{2+}$ transients amplitude induced by dantrolene on Abeta42 treated cells (light gray bar) with respect to control (dark gray bar). In neurons treated for 48 h with Abeta42 the effect of dantrolene is potentiated. (*g*) Bar graph showing that when neurons are exposed to Abeta42 for 48 h (light gray bar), dantrolene increases the firing frequency, and (*h*) cross correlation probability. These effects are more pronounced than that observed in control neurons (dark gray bar). (*i*) In neurons treated for 48 h with Abeta42 the effect of dantrolene on the amplitude of $Ca^{2+}$ transients is potentiated with respect to control (d). (*l*) MEA recording showing that in Abeta42 treated neurons dantrolene increases the frequency of spontaneous firing.

48 h of incubation with Abeta42. To finally test if RyRs are targeted by Abeta42, we measured the amount of $Ca^{2+}$ released through RyRs by stimulating neurons with the RYRs agonist caffeine (10 mM) (see Supplementary Fig. 2). We found that the average ΔF/F value was significantly (*$P < 0.05$) higher in Abeta42 treated neurons (0.9 ± 0.1, $n = 6$) with respect to control (0.3 ± 0.1, $n = 6$). We then concluded that Abeta42 increases the amount of $Ca^{2+}$ released through RyRs and that its inhibition counteracts the effects of Abeta42 on spontaneous $Ca^{2+}$ transients, firing frequency, and synchronization of neuronal hippocampal network.

## Abeta42 Oligomers Inhibit Spontaneous Firing Through BK Channels Activation

We hypothesized that $Ca^{2+}$ activated potassium channels ($IK_{Ca}$) (Marrion and Tavalin 1998) could be responsible for Abeta42 dependent inhibition of neuronal firing following the increased amplitude of spontaneous $Ca^{2+}$ transients. We first focused on small conductance potassium channels (SK channels) (see Supplementary Fig. 3) (Stocker et al. 1999; Cheong et al. 2011) observing that in control conditions the administration of the SK channels blocker apamin (200 nM) did not significantly change the firing frequency (1.5 ± 0.1 Hz [$n = 6$] in control vs. 1.4 ± 0.1 Hz [$n = 6$] with apamin [$P = 0.16$]), while the cross correlation value increased by 20.0 ± 5.0%. We then concluded that in control conditions, SK channels are mainly involved in controlling network synchronization. When SK channels were blocked in neurons previously incubated with Abeta42 (Supplementary Fig. 3), we observed that the overall firing frequency decreased from 1.2 ± 0.2 Hz ($n = 6$) to 1.0 ± 0.2 Hz, (***$P < 0.001$) while the cross correlation value was unaffected or slightly inhibited (−8.0 ± 3.0%). We concluded that SK channels inhibition does not contribute to recover the physiological firing parameters impaired by Abeta42.

Big conductance (BK) channels are involved in controlling firing rate (Storm 1987) and synaptic function (Raffaelli et al. 2004) of rat hippocampal neurons. They were blocked by paxilline (1 μM) (Marcantoni et al. 2010; Zhou and Lingle 2014), but the firing frequency of control neurons was unaffected or slightly inhibited (−8.8 ± 4.3%, $n = 5$) (Fig. 3*a*) and the cross correlation value remained unaltered (not shown). These results suggest that in control conditions BK channels are not primarily involved in governing spontaneous firing of hippocampal network. On the contrary, when neurons were incubated for 48 h with Abeta42 (Fig. 3*b*), paxilline potentiated the firing frequency by 32.1 ± 5.6% ($n = 6$) (Fig. 3*c*) without altering the cross correlation value (not shown). This result suggests that BK channels function is stimulated by Abeta42 and that they contribute to inhibit the spontaneous firing observed in hippocampal network. To test this hypothesis we performed patch clamp experiments in voltage clamp configuration (Fig. 3*d*,*e*). The maximum amplitude of $K^+$ current measured in voltage clamp experiments by depolarizing neurons from −70 to +80 mV for 400 ms was comparable among control and Abeta42 treated neurons and equal to 3.5 ± 0.4 nA ($n = 12$) in control versus 3.3 ± 0.5 nA ($n = 10$) in the presence of Abeta42. Though, the effect of paxilline was significantly potentiated by Abeta42. In particular, 14.7 ± 2.3% ($n = 12$) of the total outward potassium current is carried by BK channels in control neurons (Fig. 3*f*), while in neurons treated with Abeta42 the BK current contribution is significantly (*$P < 0.05$) increased to 23.4 ± 3.2% ($n = 10$). When the depolarizing step was preceded by stimuli of increased duration (from 10 to 90 ms) to −10 mV to open all available VGCCs (Marcantoni et al. 2010) we did not measure any further increase of the outward current (see Supplementary Fig. 4) suggesting that BK channels are maximally activated even in the absence of the above-mentioned pre-step protocol. All together these results suggest that Abeta42 stimulates the paxilline sensitive outward current carried by BK channels.

## Presynaptic BK Channels Are Upregulated by Abeta42

It is generally accepted that, in neurons, BK channels are distributed both at somatic and synaptic sites (Raffaelli et al. 2004; Martire et al. 2010). In order to understand if somatic BK channels are targeted by Abeta42, we tested if the increased intracellular $Ca^{2+}$ concentration induced by Abeta42 could affect AP duration (Marcantoni et al. 2014). We therefore performed whole cell current clamp recordings and measured the width of the first AP generated by injecting squared pulses of depolarizing currents (see Methods). In control neurons (Fig. 3*g*) paxilline widened APs and the half width increased from 1.8 ± 0.3 ms to 2.0 ± 0.3 ms ($n = 17$, *$P < 0.05$) similarly to what observed in neurons treated with Abeta42 (Fig. 3*h*) where the half width value increased from 1.6 ± 0.2 ms to 1.9 ± 0.3 ms ($n = 24$, *$P < 0.05$). We therefore concluded that somatic BK channels are not affected by Abeta42 and focused on synaptic BK channels. We first measured the spontaneous eEPSCs following AP generation (see Methods). Administration of DNQX (20 μM) together with picrotoxin completely blocked eEPSCs (not shown) thus suggesting that they are mainly mediated by AMPARs activation. In control neurons (Fig. 3*i*), neither the amplitude (Fig. 3*l*), nor the frequency (Fig. 3*m*) of AMPA dependent eEPSCs were affected by paxilline. The average amplitude was, respectively, −12.8 ± 0.2 pA in control and −12.4 ± 0.2 pA with paxilline ($n = 12$, $P = 0.14$), while the inter event interval (IEI) was 147.6 ± 3.3 ms and 155.7 ± 4.5 ms with paxilline ($P = 0.13$). We then concluded that in physiological conditions, while BK channels contribute to AP duration, they are not involved in controlling the AMPA dependent glutamatergic synapses. In good agreement with the decreased firing activity induced by Abeta42 administration (Fig. 1*b*–*d*), when we compared control neurons with those treated with Abeta42 (Fig. 3*n*), the eEPSCs amplitude of these latter increased significantly to −21.7 ± 0.6 pA ($n = 10$, Fig.3*o*) and was not sensitive to the presence of paxilline (−21.1 ± 0.6 pA, $P = 0.48$). IEI values were significantly higher as well (189.3 ± 7.7 ms, Fig. 3*p*) and with paxilline they decreased to 131.3 ± 5.9 ms (***$P < 0.001$). All together these results suggest that, being Abeta42 able to alter both IEI and amplitude of eEPSCs, it targets AMPA dependent glutamatergic synapses at presynaptic and postsynaptic sites. Being only the IEI values affected by the presence of paxilline, we concluded that presynaptic BK channels dependent current is stimulated by Abeta42.

Although in control neurons BK channels are not involved in controlling spontaneous firing (Fig. 3*a*), we tested the hypothesis that these latter could be recruited when the amount of $Ca^{2+}$ released by RyRs increased, thus determining glutamatergic AMPA dependent current inhibition. To this purpose we measured electrically evoked monosynaptic AMPA dependent glutamatergic EPSCs (eEPSCs) in control conditions and after administration of caffeine and paxilline. These 2 compounds were used for, respectively, stimulate $Ca^{2+}$ release from RyRs and inhibit BK channels. We observed that activation of RyRs by caffeine inhibited eEPSCs by 64% (from 152.0 ± 73.0 pA, $n = 28$ to 54.2 ± 23.9 pA, $n = 8$, *$P < 0.05$ by ANOVA) (Fig. 4*a*,*d*). Because this effect was abolished by paxilline, we concluded that, when $Ca^{2+}$ released by RyRs increases, it activates BK

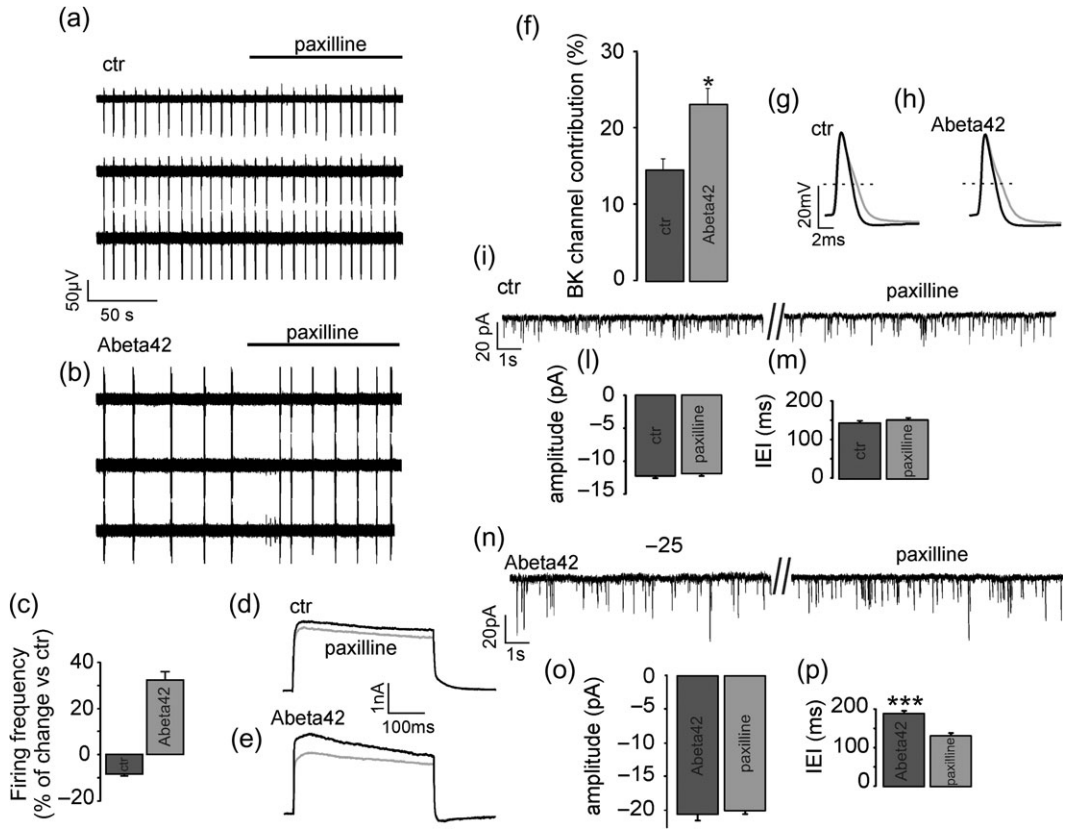


**Figure 3.** (*a*) Three representative channels from the same MEA showing that while spontaneous firing is not altered by paxilline (1 μM) in control neurons, it is increased (*b*) in those treated for 48 h with Abeta42. (*c*) Bar graph summarizing that firing frequency of cultured hippocampal network is unaffected or slightly inhibited by paxilline in control neurons (dark gray bar), while it is increased in Abeta42 treated neurons (light gray bar). (*d*) Paxilline (light gray trace) inhibits the total outward $K^+$ current (black trace) in control. (*e*) The inhibition of $K^+$ current induced by paxilline is potentiated after 48 h of incubation with Abeta42. (*f*) Bar graph summarizing the contribution of BK activated current with respect to the total amount of $K^+$ current activated in hippocampal neurons in control conditions (dark gray bar) and in presence of Abeta42 (light gray bar). (*g*) Paxilline (light gray trace) broadens the action potential shape in control neurons (black trace). The effect is comparable to that measured in neurons incubated for 48 h with Abeta42 (*h*). The dotted lines in g, h correspond to membrane potential of 0 mV. (*i*) Representative recording of AMPA eEPSCs elicited by spontaneous APs in control conditions. Paxilline does not modify neither the amplitude (*l*) nor the frequency (*m*) of eEPSCs following AP generation. (*n*) In neurons treated with Abeta42 paxilline does not alter eEPSCs amplitude (*o*) but decreases the inter event interval (IEI) (*p*).

channels which in turn inhibit AMPA dependent eEPSCs. We next tested whether in control neurons the inhibition of RyRs and/or BK channels could affect AMPA dependent synaptic transmission. Monosynaptic eEPSCs were first measured in the presence of paxilline (Fig. 4*b*,*d*) and their average amplitude (142.0 ± 19.3 pA, $n = 20$) was comparable to control conditions, unlike to what observed in Abeta42 treated neurons (Fig. 4*c*,*d*), where the average eEPSCs amplitude (177.8 ± 18.6 pA, $n = 28$) was increased by paxilline to 291.7 ± 70.6 pA ($n = 10$, $^*P < 0.05$). Dantrolene (Fig. 4*b*,*e*) did not change the average eEPSCs amplitude measured in control neurons (145.6 ± 21.0, $n = 15$), that instead increased to 368.3 ± 70.4 pA ($n = 11$, $^*P < 0.05$) after incubation with Abeta42 (Fig. 4*c*,*e*). Simultaneous administration of dantrolene together with paxilline did not alter significantly the amplitude of eEPSCs in control neurons (168.0 ± 42.0 pA, $n = 15$, Fig. 4*b*,*e*), but abolished the potentiating effect observed in Abeta42 treated neurons, making the average eEPSCs amplitude (141.2 ± 37.2 pA, $n = 6$) comparable to that measured before RyRs and BK channels inhibition (Fig. 4*c*,*e*). These results confirm that Abeta42 inhibits the amplitude of AMPA dependent eEPSCs by stimulating RyRs and BK channels function.

## NMDARs Are Inhibited by Abeta42 Oligomers

DNQX (20 μM) and TTX (0.3 μM) completely abolished spontaneous $Ca^{2+}$ transients (Fig. 5*a*), suggesting that AMPARs and voltage gated $Na^+$ channels control $Ca^{2+}$ oscillations by governing, respectively, synaptic and somatic dependent depolarizations. Alternatively to AMPARs, NMDARs as well can be activated by glutamate released at excitatory synapses and mediate $Ca^{2+}$ entering into neurons. We therefore focused on the mechanisms of $Ca^{2+}$ entry through NMDARs by measuring their contribution in the regulation of $Ca^{2+}$ influx both in control (Fig. 5*a*) and in the presence of Abeta42 (Fig. 5*b*). The selective NMDARs blocker APV (50 μM) inhibited $Ca^{2+}$ transients amplitude in control neurons by 68.5 ± 7.2% and this effect was more pronounced ($^{***}P < 0.001$) than in Abeta42 treated neurons (47.7 ± 4.2% of inhibition) (Fig. 5*c*). We next tested the effect of APV on spontaneous firing observing that it was inhibited by 59.8 ± 2.6% ($n = 5$) in control neurons (Fig. 5*d*,*f*). This effect was significantly ($^{***}P < 0.001$) reduced to 33.6 ± 7.3% ($n = 4$) in Abeta42 treated neurons (Fig. 5*e*,*f*). Cross correlation analysis (Fig. 5*g*) showed that APV increased network synchronization by 25.9 ± 5.5% in control neurons and that this effect was significantly ($^{***}P < 0.001$) more pronounced in the presence of Abeta42 (89.7 ± 12.8%). All together these results

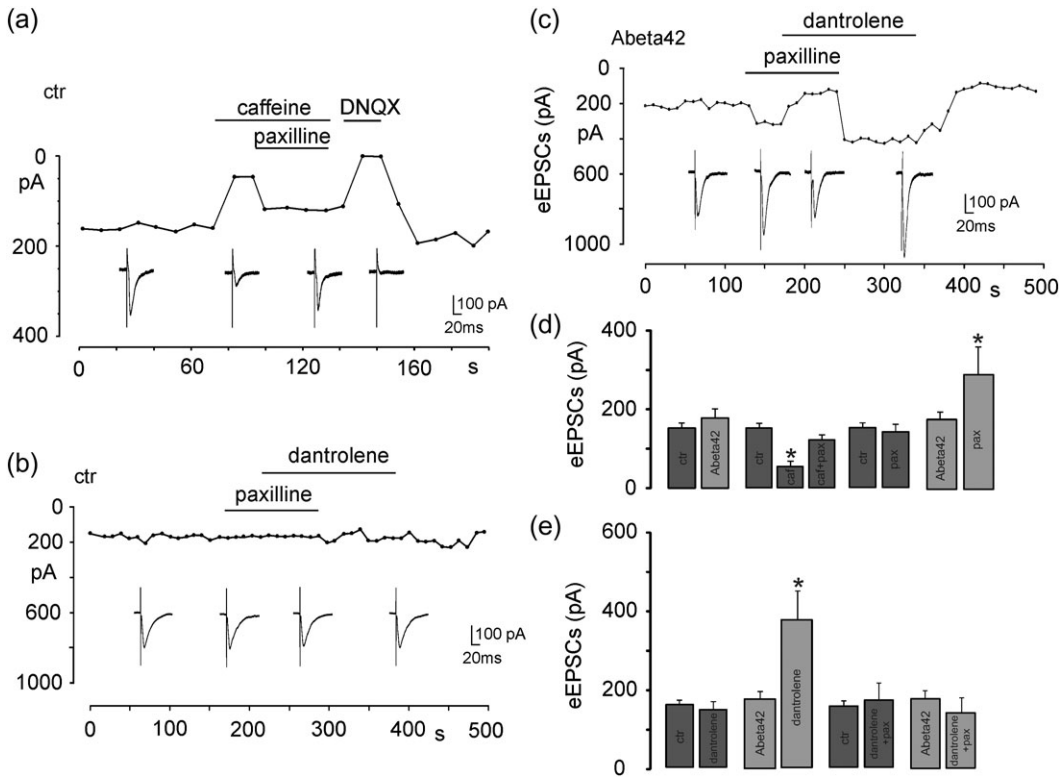


**Figure 4.** (*a*) In control neurons, electrically evoked AMPA eEPSCs amplitude is significantly inhibited by caffeine (10 mM) while paxilline abolishes this effect, (*b*) Administration of paxilline and dantrolene simultaneously or separately does not change the average amplitude of eEPSCs measured in control neurons. (*c*) After incubation with Abeta42 oligomers for 48 h eEPSCs amplitude increases when paxilline or dantrolene are administered separately. This effect is abolished when the 2 compounds are administered together. (*d*) Bar graphs comparing the average eEPSCs amplitude in control neurons (dark gray bars) with that measured in neurons incubated 48 h with Abeta42 (light gray bars). The average eEPSCs amplitudes of the 2 populations are comparable and are inhibited by caffeine in control neurons. This effect is abolished by paxilline. In control neurons paxilline alone does not interfere with the average eEPSCs amplitude, which is increased in neurons previously incubated with Abeta42. (*e*) Bar graphs summarizing the effect of dantrolene alone and together with paxilline in control neurons (dark gray bars) and in those incubated for 48 h with Abeta42 (light gray bars). eEPSCs amplitude from control neurons are not affected by dantrolene administered alone or together with paxilline. Dantrolene potentiates the eEPSCs amplitude in neurons previously incubated with Abeta42. This potentiating effect induced by dantrolene is abolished by paxilline.

suggest that Abeta42 inhibits NMDARs and that these latter are important for governing both spontaneous network depolarizations and $Ca^{2+}$ oscillations.

### Abeta42 Inhibits $Ca^{2+}$ Entry Through VGCCs

Together with NMDARs, VGCCs regulate $Ca^{2+}$ entry through plasma membrane (Alford et al. 1993; Goussakov et al. 2010). We found that when cadmium (200 μM) was added to extracellular medium together with APV, it completely abolished intracellular $Ca^{2+}$ oscillations (Fig. 6*a*), suggesting that, in control neurons, VGCCs together with NMDARs are important for governing spontaneous $Ca^{2+}$ transients. We therefore performed patch clamp experiments to verify whether Abeta42 affect VGCCs, by considering both L- and non-L-type channels known to be largely expressed in hippocampal neurons (Baldelli et al. 2000, 2002). In control neurons (Fig. 6*b*) after 11–14 DIV the total $Ca^{2+}$ current at −10 mV in 2 mM $Ca^{2+}$ was −692.8 ± 80.5 pA ($n$ = 24) (Fig. 6*c*). Addition of 3 μM nifedipine reduced the peak current amplitude to −430.3 ± 55.6 pA (Fig. 6*b*,*c*) indicating that LTCCs contribute to 38% of total $Ca^{2+}$ current (256.1 ± 37.4 pA), while the remaining 62% of total $Ca^{2+}$ current is carried by non-LTCCs. In the presence of Abeta42 the amount of total $Ca^{2+}$ current (Fig. 6*d*) significantly decreased to −284.5 ± 40.0 pA ($n$ = 17, $^{***}P < 0.001$). When LTCCs were blocked with nifedipine, the remaining $Ca^{2+}$ current was −162.6 ± 31.8 pA (Fig. 6*c*, *d*). The contribution of LTCCs was slightly but not significantly increased to 42.6% and the remaining 57.4% of the total $Ca^{2+}$ current carried by non-LTCCs was comparable to that of control neurons. We then concluded that Abeta42 oligomers decreased the amplitude of $Ca^{2+}$ current carried by VGCCs without altering the proportion between L and non-LTCCs.

## Discussion

We studied the effects of APP derived protein Abeta42 on neuronal network excitability. Our results suggest that, after 48 h of incubation, Abeta42 inhibits spontaneous firing and increases $Ca^{2+}$ transients amplitude. We suggest that Abeta42 is responsible for remodeling intracellular $Ca^{2+}$ homeostasis as a consequence of RyRs stimulation followed by NMDARs and VGCCs inhibition. All together these effects contribute to reduce the network excitability through BK channels activation and inhibition of AMPA dependent synaptic current. Physiological excitatory parameters are partially restored through the inhibition of RyRs or BK channels suggesting that their selective target could be useful for treating early symptoms of AD.

### Inhibition of Spontaneous Firing by Abeta42

Our previous reports (Gavello et al. 2012; Allio et al. 2015) show that primary cultures of hippocampal neurons generate spontaneous bursts of APs recorded extracellularly by means of MEAs.

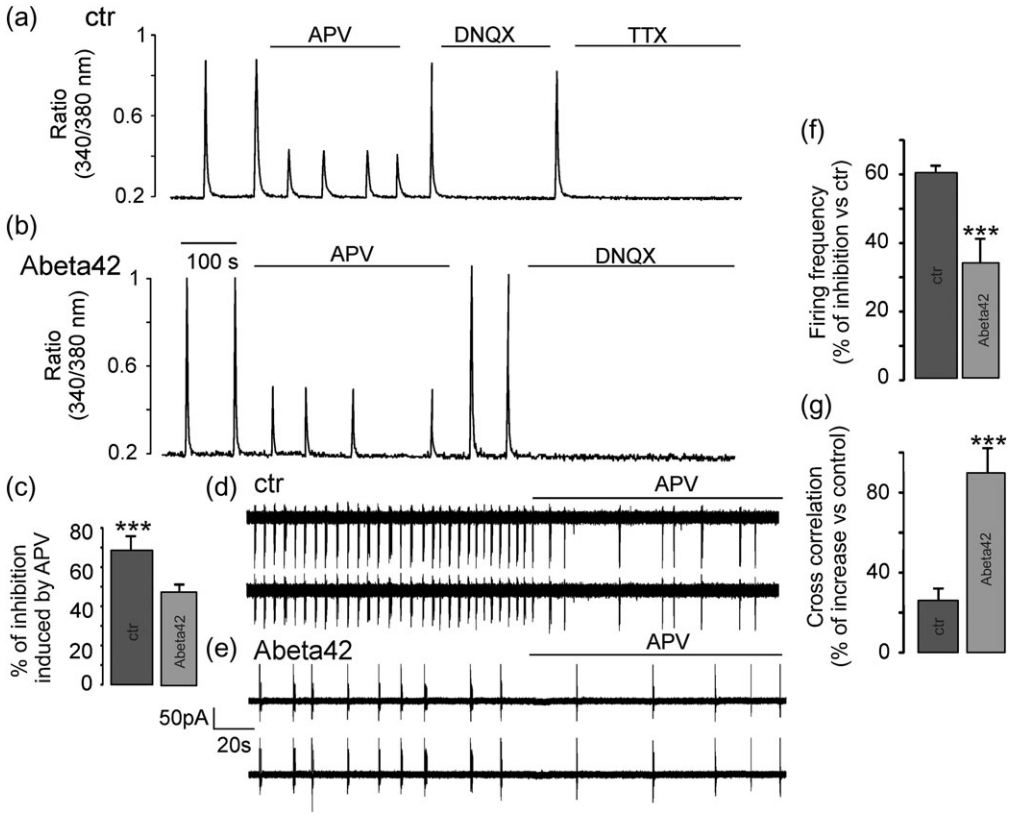


**Figure 5.** (*a*) DNQX completely abolishes $Ca^{2+}$ oscillations both in control conditions and in neurons treated with Abeta42 oligomers (*b*). NMDARs contribute to $Ca^{2+}$ oscillations in control (a) where APV inhibits the peak of $Ca^{2+}$ transients. This effect is reduced in neurons treated with Abeta42 (b). The inhibition of somatic action potentials with TTX abolishes the $Ca^{2+}$ oscillations as well (a). (*c*) Bar graph showing that Abeta42 (light gray bar) significantly reduces the effect of APV with respect to control (dark gray bar). (*d*) APV inhibits spontaneous firing of hippocampal network. This effect is reduced by Abeta42 (*e*). (*f*) Bar graph summarizing the inhibition of spontaneous firing frequency induced by APV in control (dark gray bar) and in neurons incubated with Abeta42. The inhibitory effect is significantly depressed by Abeta42. (*g*) Bar graph summarizing the potentiating effect of APV on network synchronization measured by considering the cross correlation probability. Although APV inhibits the average firing frequency (*f*) it increases network synchronization more markedly in neurons treated with Abeta42 than in control.

Here, we show that spontaneous firing depends on both somatic and synaptic excitability (Fig. 1*a*). In particular, we clearly define the degree of importance of both glutamatergic and GABAergic synapses in governing network excitability and show that, while it is completely abolished by blocking glutamatergic AMPARs, it is only partially altered when GABAergic (Fig. 1*c*) and NMDARs (Fig. 5*d*) are inhibited. Here, we focused on the role of glutamatergic AMPA-dependent synapses to regulate spontaneous firing. However, future experiments will be needed for clarify any specific effect induced by Abeta42 on the GABAergic counterpart.

It is already well established that in AD the mechanisms of synaptic transmission are impaired (Ye et al. 2010; Chong et al. 2011), but recent reports suggest that intrinsic neuronal excitable properties are modified too (Marcantoni et al. 2014; Tamagnini et al. 2015). These effects are often contradictory and not well understood, probably because many causal agents that contribute to AD onset exist and many animal models have been proposed to be suitable for studying this pathology. A great quantity of data comes from experiments on AD transgenic animals that exhibit Abeta accumulation (Marchetti and Marie 2011). Among various forms of Abeta oligomers, Abeta42 is considered particularly toxic for neurons (Lambert et al. 1998). Here, we focus on its effects on both spontaneous network excitability and $Ca^{2+}$ oscillations.

One of the major issues concerning the use of Abeta42 is represented by its tendency to aggregate during time (Dahlgren et al. 2002; Puzzo et al. 2009) and to exert different effects depending on its concentration that in turn affects the aggregation process as well (Mucke and Selkoe 2012). We therefore identified the main structure and concentration of Abeta42 responsible for neuronal dysfunction. We suggest that Abeta42 oligomers, rather than fibrils, are the main responsible for neuronal dysfunction. This conclusion agrees with most of the data presented in literature, but contrasts with others (Minkeviciene et al. 2009) which identify Abeta42 fibrils as the main cause of the increased neuronal excitability observed. Being our experimental conditions significantly different from those reported by Minkeviciene et al. (e.g., Abeta42 concentration and time of exposure), we concluded that these conflicting results cannot be compared and we do not exclude that high concentrations (100 μM) of fibrils of Abeta42 during shorter period of incubations (1 h) could increase neuronal excitability. Moreover, the Abeta42 dependent effects here described could be presumably influenced by the presence of other Abeta peptides such as Abeta40. These latter may in turn influence the Abeta aggregation process as already reported (Kuperstein et al. 2010). Future experiments will be necessary to clarify this issue. Finally, new insights about the effects of Abeta42 are provided in this work by MEA recordings: We demonstrate that the spontaneous neuronal firing is inhibited (Fig. 1*b*,*d*), as well as the number and the duration of bursts (Fig. 1*f*,*g*). Burst activity is critical for neuronal function since during those prolonged

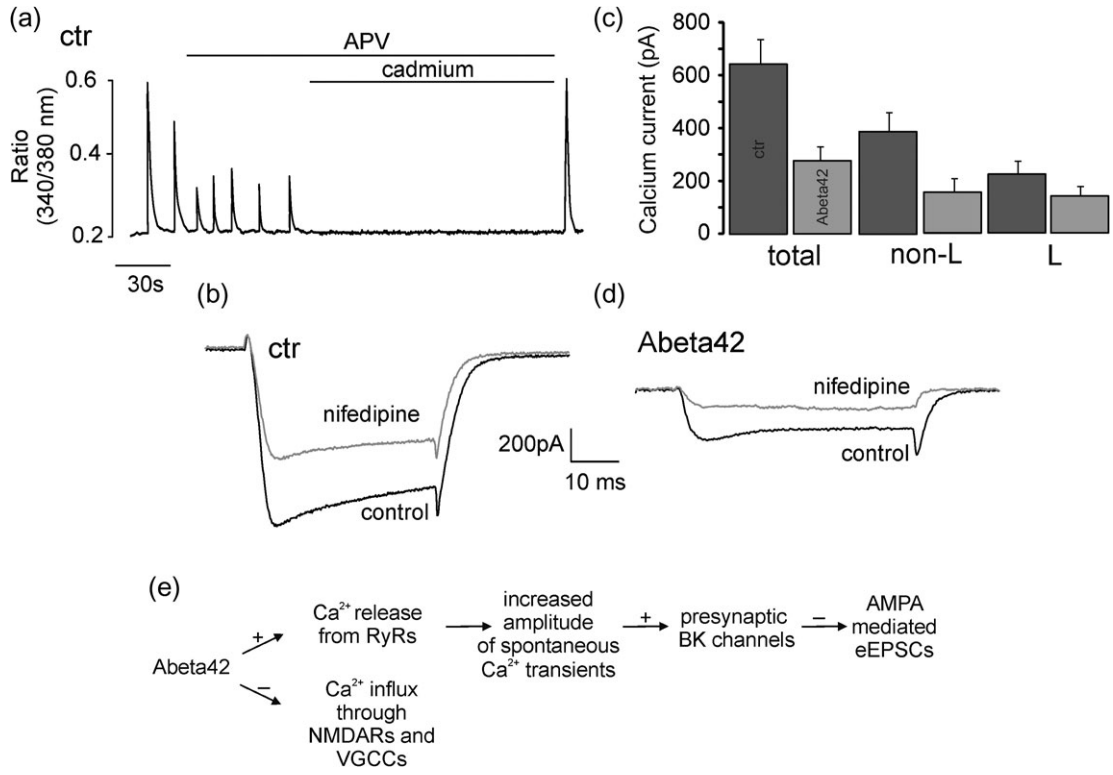


**Figure 6.** (*a*) In control neurons cadmium together with APV completely abolishes intracellular $Ca^{2+}$ oscillations. (*b*) In control neurons nifedipine (light gray trace) reduces by 38% the total $Ca^{2+}$ current (black trace). (*c*) Bar graph showing the almost proportional halving of total, non-L type, and L-type $Ca^{2+}$ currents induced by incubation of neurons with Abeta42 (light gray bars) when compared with control conditions (dark gray bars). (*d*) Similarly to what observed in control neurons, nifedipine (light gray trace) inhibits by 43% the total $Ca^{2+}$ current (black trace) after incubation with Abeta42. (*e*) Chart summarizing the main results obtained: Abeta42 increases intracellular $Ca^{2+}$ concentration of primary cultured hippocampal and inhibits neuronal network excitability by mainly increasing the amount of $Ca^{2+}$ released through RyRs that in turn inhibits glutamatergic AMPA dependent synapses through activation of BK channels. Finally, a further contribution to firing inhibition is given by the decreased $Ca^{2+}$ influx through NMDARs and VGCCs induced by Abeta42.

excitatory periods, typical of mature networks, $Ca^{2+}$ enters into neurons and regulates many neuronal activities as well as neurotransmitter release. Furthermore, we clearly show that Abeta42 inhibits network synchronization (Fig. 1*h*), causing, in this way, the reduction of effectiveness of synaptic input (Marcantoni et al. 2014).

## ABeta42 Oligomers Stimulate Spontaneous Calcium Transients by Mainly Targeting RYRs

As already observed in different neurons (Murphy et al. 1992; van den Pol et al. 1992; Bacci et al. 1999; Wang et al. 2009) network of primary cultured hippocampal neurons generate spontaneous $Ca^{2+}$ transients (Fig. 2*a*) of longer duration than bursts of APs. Here, we show that bursts of APs occur on average 10-folds faster than $Ca^{2+}$ transients (hundred ms duration versus seconds), suggesting that several bursts of APs occur during one single $Ca^{2+}$ transient. We also suggest that a correlation between $Ca^{2+}$ transient amplitudes and firing frequency exists and the general rule is that by increasing the amplitude of $Ca^{2+}$ transients the firing frequency is inhibited. Several studies demonstrate that $Ca^{2+}$ dyshomeostasis is early observed in AD and it can contribute to generate synaptic dysfunction. We aimed at evaluating the effect of ABeta42 on spontaneous $Ca^{2+}$ transients and how these could be correlated with altered neuronal network excitability. To this regard, it has been proposed that Abeta42 could create pores into the plasma membrane and that these latter could contribute to determine $Ca^{2+}$ dyshomeostasis phenomena (Demuro et al. 2011). Our experiments show that neither the basal intracellular $Ca^{2+}$ concentration (Fig. 2*b*), nor the $R_m$ value are altered by Abeta42. Thus we can conclude that, in our experimental conditions, Abeta42 does not form $Ca^{2+}$ permeable pores. Increasing evidences support the idea that RyRs activity is upregulated in AD, but most of the studies are limited to transgenic mice (Oules et al. 2012; Chakroborty et al. 2013) and only few reports propose an effect of Abeta42 on RyRs (Supnet et al. 2006; Lazzari et al. 2014). Here, by blocking RyRs with dantrolene (Fig. 2) and stimulating them with caffeine (Supplementary Fig. 2) we clearly show their increased function induced by Abeta42. As already observed in thalamocortical neurons (Cheong et al. 2011), we propose that under basal physiological conditions the spontaneous firing network is not affected by $Ca^{2+}$ released through RyRs. On the other hand, it is known that when the duration (Cheong et al. 2011) or the frequency (Riquelme et al. 2010) of electrical stimuli increases, the amount of $Ca^{2+}$ released by RyRs increases as well and becomes involved in setting the neuronal firing frequency. Similarly to what above described, here we suggest that when ABeta42 targets RyRs the amount of intracellular $Ca^{2+}$ concentration increases enough to inhibit firing network. To support this hypothesis, we finally demonstrate that dantrolene is able to reverse the inhibitory effects of Abeta42 on firing activity and synchronization of hippocampal network. Currently, the precise effect of Abeta42 on RyRs is still to be elucidated. Future experiments are needed to characterize whether Abeta42 is responsible for the increased $Ca^{2+}$ loading

of intracellular stores or for the increased number and/or conductance of available RyRs. To this regard, it has been recently shown (Barucker et al. 2014) that, already after 30 min of incubation, Abeta42 is found in the nucleus and interferes with gene transcription. We therefore cannot exclude the hypothesis that after 48–72 h of incubation Abeta42 could interfere with RyRs gene transcription process. It is worth noticing that here we do not consider the effect of Abeta42 on $IP_3$ receptors. Many reports suggest that during AD the amount of $Ca^{2+}$ released through $IP_3$ receptors is increased as well (Stutzmann et al. 2004; Oules et al. 2012; Chakroborty et al. 2013), but other recent reports indicate that their function is inhibited by Abeta42 (Lazzari et al. 2014). Despite these contrasting results, it is well accepted that $Ca^{2+}$ released through $IP_3$ receptors concurs to the activation of RyRs and that dantrolene treatment suppresses $Ca^{2+}$ release from both receptors (Chakroborty et al. 2013) thus confirming the effectiveness of dantrolene during AD onset.

## BK Channels Are Targeted by Abeta42

Our data demonstrate that Abeta42, besides inhibiting neuronal firing and synchronization, increases the amplitude of intracellular $Ca^{2+}$ oscillations, thus suggesting a possible involvement of $Ca^{2+}$ activated potassium channels ($IK_{Ca}$). Two classes of $IK_{Ca}$ with different affinity for $Ca^{2+}$ exist. They are represented by $Ca^{2+}$ dependent small conductance (SK) and voltage and $Ca^{2+}$ dependent large conductance (BK) $K^+$ channels (Fakler and Adelman 2008). The former govern firing rate, adaptation, regularity of APs firing. Their block prevents the repolarization at the end of the single AP, thus decreasing the number of $Na^+$ channels available for the next spike, increasing AP width and bringing neuron to a depolarizing block condition (Vandael et al. 2015). This mechanism could explain the inhibition of firing frequency and synchronism induced by apamin on spontaneous firing of hippocampal neurons treated with Abeta42 (Supplementary Fig. 3), similarly to what observed in AD mice models where the synaptic function is altered by upregulation of SK channels (Chakroborty et al. 2012). However, since SK channels inhibition does not contribute to recover the physiological firing parameters impaired by Abeta42, therefore it is reasonable to assume they do not represent a promising target for restoring impaired neuronal function. We next focused on the role of BK channels, characterized by lower degree of affinity for $Ca^{2+}$ with respect to SK, being activated by higher intracellular $Ca^{2+}$ concentration (more than 10 μM) (Vandael et al. 2015). For these reasons, in neurons or neuronal like cells, BK channels are co-localized with the $Ca^{2+}$ source mainly represented either by $Ca^{2+}$ channels (Marrion and Tavalin 1998; Marcantoni et al. 2010; Vandael et al. 2010), or by RyRs as well (Chavis et al. 1998; Beurg et al. 2005). It is generally accepted that BK channels are located at both somatic and synaptic sites (Hu et al. 2001) and are, respectively, important for controlling the AP shape (Storm 1987) and the neurotransmitter release (Raffaelli et al. 2004; Martire et al. 2010). Similarly to what already described (Hu et al. 2001), here we show that in control neurons BK channels contribute little to the total $K^+$ activated current (Fig. 3*d*) even when increased amount of $Ca^{2+}$ enters into neurons (Supplementary Fig. 4). We therefore conclude that they regulate the AP shape (Fig. 3*g*) but are scarcely involved in controlling spontaneous firing of hippocampal network (Fig. 3*a*) and do not regulate neurotransmitter release (Figs 3*i* and 4*b*), unless RyRs are strongly activated (Fig. 4*a*). On the contrary, in the presence of Abeta42, the increased amount of intracellular $Ca^{2+}$ concentration potentiates BK channels activation (Fig. 3*e*,*f*) and this effect is specific for the presynaptic (Figs 3*n* and 4*c*), but not somatic (Fig. 3*h*) compartment. We in fact show that paxilline increases the frequency (Fig. 3*p*), but not the amplitude of spontaneous eEPSCs following AP generation (Fig. 3*o*) and increases the amplitude of electrically evocked eEPSCs (Fig. 4*e*), while the AP duration is comparable to that measured in control neurons (Fig. 3*g*,*h*). Further experiments will be necessary to understand the molecular mechanism responsible for BK channels activation induced by Abeta42 since we cannot exclude that the density and/or the conductance of these channels are increased. To this regard, a recent report (Donnelier et al. 2015) suggests that Abeta42 does not increase the expression of the BK α subunit expression reinforcing the hypothesis of increased BK channels conductance. Finally, the experiments here discussed do not only demonstrate the activation of BK current by Abeta42, in good agreement with previous findings (Ye et al. 2010). They also indicate the presence of a strong link between the increased amount of $Ca^{2+}$ released by RyRs, the activation of BK channels and inhibition of the amplitude of glutamatergic AMPA dependent current (Fig. 4*a*). These overall effects could be responsible for decreasing the rate of glutamate release and in turn the rate of spontaneous firing of hippocampal network. It is noteworthy that while the frequency of eEPSCs in neurons treated with ABeta42 is significantly reduced when compared with control conditions, their amplitude is higher (Fig. 3*l*,*o*). We therefore conclude that presynaptic BK channels could be preferentially coupled with RyRs and that postsynaptic AMPARs function is upregulated by ABeta42, but the specific effects induced by Abea42, respectively, at presynaptic and postsynaptic glutamatergic compartment are still to be investigated, as well as the molecular pathway that determines the increased amount of $Ca^{2+}$ released by RyRs. Finally, we cannot also exclude that a coupling between $IP_3$ receptors and BK channels could exist, but, while these latter are mainly distributed at somatic region, RyRs prefer synaptic sites (Goussakov et al. 2010; Chakroborty et al. 2012) where BK channels are upregulated. All together these results strongly indicate BK channels as a target for treating early symptoms of AD.

## NMDARs and VGCCs Are Inhibited by Abeta42

NMDARs are important for controlling spontaneous $Ca^{2+}$ transients and it is well accepted that they are inhibited during aging (Thibault et al. 2007) and in AD (Yu et al. 2009). This mechanism of $Ca^{2+}$ influx is thought to be involved in governing neuronal plasticity, learning and memory processes (Malenka et al. 1988) that are known to be impaired in AD (LaFerla 2002). Our data add new insights about the effect of Abeta42 in the regulation of intracellular $Ca^{2+}$ concentration by NMDARs. First, we demonstrate that $Ca^{2+}$ transients recorded in cultured hippocampal neurons depend by both somatic APs generation and activation of glutamatergic synapses (Fig. 5*a*). We in fact show that TTX administration abolishes completely $Ca^{2+}$ oscillations and the same is observed by blocking AMPARs through DNQX. Our data suggest that AMPARs are essential for spontaneous generation of $Ca^{2+}$ transients while NMDA contribute only partially to this phenomenon and confirm what already observed in rat derived hippocampal neurons (Bacci et al. 1999). The involvement of NMDARs in governing spontaneous firing of hippocampal network (Fig. 5*d*) has been studied too. Our results show that their inhibition contributes only in part to the recovery of neuronal firing properties impaired by Abeta42, by increasing network

synchronization, but not firing frequency, thus suggesting that the effectiveness of therapies for AD treatment based on NMDARs blockers actually employed mainly depends on their ability to preserve the neuronal network synchronism. We finally observed that the effect of APV on $Ca^{2+}$ transients and firing is less pronounced in the presence of Abeta42 (Fig. 5*b*,*c*). Even if future experiments will be needed for clarifying this issue, all together these results suggest that NMDARs and the spontaneous firing activity of hippocampal networks are inhibited by Abeta42.

Hippocampal pyramidal neurons express high densities of LTCCs in the cell body and proximal dendrites. They contribute to increase $Ca^{2+}$ entry following NMDARs activation and together with NMDARs are involved in the control of $Ca^{2+}$ influx and neuronal plasticity in hippocampus (Westenbroek et al. 1990). In addition, VGCCs are important to regulate the excitability of neurons (Bean 2007) or neuronal like cells (Marcantoni et al. 2009, 2010; Vandael et al. 2015). Several reports indicate that their contribution to $Ca^{2+}$ entry through plasma membrane increases during age when they are upregulated (Thibault et al. 2007; Yu et al. 2009). LTCCs upregulation has been frequently observed during AD (Wang and Mattson 2013), but opposing evidences suggest that they can be inhibited as well (Thibault et al. 2012). This underlies the variability of effects on $Ca^{2+}$ homeostasis observed in AD probably correlated with the multifactorial causes of the pathology together with different responses of the brain region of interest. Here, we show their involvement in the spontaneous generation of $Ca^{2+}$ transients (Fig. 6*a*) and the inhibition of both L and non-LTCCs isoforms (Fig. 6*b*–*d*) induced by Abeta42. In conclusion, the present work clarifies the effects of Abeta42 on neuronal function and, by focusing on the mechanisms that regulate $Ca^{2+}$ oscillations, firing, synaptic function, correlates data from neuronal networks with those on isolated neurons. We suggest that Abeta42 increases the amplitude of $Ca^{2+}$ transients, decreases the firing rate and network synchronization by mainly increasing RyRs and BK channels functions and inhibiting NMDARs and VGCCs (Fig. 6*e*). The modulation of these targets would represent a promising strategy for early treatment of AD. We wish finally to point out that previous results obtained by our group (Marcantoni et al. 2014) revealed that excitatory profile of neurons from LEC is early altered during AD onset. These results indicate that sensory inputs involved in memory formation, including olfactory information processing conveyed by LEC to hippocampus, might be early compromised and suggest how new diagnostic methods for an early identification of AD should be addressed.

## Supplementary Material

Supplementary material is available at *Cerebral Cortex* online.

## Funding

MIUR (Euro-Mediterranean PRES project to A.M., PRIN 2010/2011 project 2010JFYFY2 to E.C.); local funds from University of Torino to A.M. and V.C.; Telethon Foundation (grant # GGP15110) to E.C.

## Notes

We thank Dr. A. Allio for critical reading and discussion. *Conflict of Interest*: None declared.

## References

Alford S, Frenguelli BG, Schofield JG, Collingridge GL. 1993. Characterization of Ca2+ signals induced in hippocampal CA1 neurones by the synaptic activation of NMDA receptors. J Physiol. 469:693–716.

Allio A, Calorio C, Franchino C, Gavello D, Carbone E, Marcantoni A. 2015. Bud extracts from Tilia tomentosa Moench inhibit hippocampal neuronal firing through GABA and benzodiazepine receptors activation. J Ethnopharmacol. 172:288–296.

Arnold FJ, Hofmann F, Bengtson CP, Wittmann M, Vanhoutte P, Bading H. 2004. Microelectrode array recordings of cultured hippocampal networks reveal a simple model for transcription and protein synthesis-dependent plasticity. J Physiol. 564:3–19.

Bacci A, Verderio C, Pravettoni E, Matteoli M. 1999. Synaptic and intrinsic mechanisms shape synchronous oscillations in hippocampal neurons in culture. Eur J Neurosci. 11:389–397.

Baldelli P, Forni PE, Carbone E. 2000. BDNF, NT-3 and NGF induce distinct new Ca2+ channel synthesis in developing hippocampal neurons. Eur J Neurosci. 12:4017–4032.

Baldelli P, Hernandez-Guijo JM, Carabelli V, Carbone E. 2005. Brain-derived neurotrophic factor enhances GABA release probability and nonuniform distribution of N- and P/Q-type channels on release sites of hippocampal inhibitory synapses. J Neurosci. 25:3358–3368.

Baldelli P, Novara M, Carabelli V, Hernandez-Guijo JM, Carbone E. 2002. BDNF up-regulates evoked GABAergic transmission in developing hippocampus by potentiating presynaptic N- and P/Q-type Ca2+ channels signalling. Eur J Neurosci. 16: 2297–2310.

Barucker C, Harmeier A, Weiske J, Fauler B, Albring KF, Prokop S, Hildebrand P, Lurz R, Heppner FL, Huber O, et al. 2014. Nuclear translocation uncovers the amyloid peptide Abeta42 as a regulator of gene transcription. J Biol Chem. 289:20182–20191.

Bean BP. 2007. The action potential in mammalian central neurons. Nat Rev Neurosci. 8:451–465.

Benilova I, Karran E, De Strooper B. 2012. The toxic Abeta oligomer and Alzheimer's disease: an emperor in need of clothes. Nat Neurosci. 15:349–357.

Beurg M, Hafidi A, Skinner LJ, Ruel J, Nouvian R, Henaff M, Puel JL, Aran JM, Dulon D. 2005. Ryanodine receptors and BK channels act as a presynaptic depressor of neurotransmission in cochlear inner hair cells. Eur J Neurosci. 22:1109–1119.

Chakroborty S, Briggs C, Miller MB, Goussakov I, Schneider C, Kim J, Wicks J, Richardson JC, Conklin V, Cameransi BG, et al. 2013. Stabilizing ER Ca2+ channel function as an early preventative strategy for Alzheimer's disease. PLoS One. 7:e52056.

Chakroborty S, Kim J, Schneider C, Jacobson C, Molgo J, Stutzmann GE. 2012. Early presynaptic and postsynaptic calcium signaling abnormalities mask underlying synaptic depression in presymptomatic Alzheimer's disease mice. J Neurosci. 32:8341–8353.

Charkhkar H, Meyyappan S, Matveeva E, Moll JR, McHail DG, Peixoto N, Cliff RO, Pancrazio JJ. 2015. Amyloid beta modulation of neuronal network activity in vitro. Brain Res. 1629:1–9.

Chavis P, Ango F, Michel JM, Bockaert J, Fagni L. 1998. Modulation of big K+ channel activity by ryanodine receptors and L-type Ca2+ channels in neurons. Eur J Neurosci. 10:2322–2327.

Cheong E, Kim C, Choi BJ, Sun M, Shin HS. 2011. Thalamic ryanodine receptors are involved in controlling the tonic firing

of thalamocortical neurons and inflammatory pain signal processing. J Neurosci. 31:1213–1218.
Chong SA, Benilova I, Shaban H, De Strooper B, Devijver H, Moechars D, Eberle W, Bartic C, Van Leuven F, Callewaert G. 2011. Synaptic dysfunction in hippocampus of transgenic mouse models of Alzheimer's disease: a multi-electrode array study. Neurobiol Dis. 44:284–291.
Dahlgren KN, Manelli AM, Stine WB Jr, Baker LK, Krafft GA, LaDu MJ. 2002. Oligomeric and fibrillar species of amyloid-beta peptides differentially affect neuronal viability. J Biol Chem. 277:32046–32053.
Demuro A, Smith M, Parker I. 2011. Single-channel Ca(2+) imaging implicates Abeta1-42 amyloid pores in Alzheimer's disease pathology. J Cell Biol. 195:515–524.
Donnelier J, Braun ST, Dolzhanskaya N, Ahrendt E, Braun AP, Velinov M, Braun JE. 2015. Increased Expression of the Large Conductance, Calcium-Activated K+ (BK) Channel in Adult-Onset Neuronal Ceroid Lipofuscinosis. PLoS One. 10:e0125205.
Fakler B, Adelman JP. 2008. Control of K(Ca) channels by calcium nano/microdomains. Neuron. 59:873–881.
Gavello D, Rojo-Ruiz J, Marcantoni A, Franchino C, Carbone E, Carabelli V. 2012. Leptin counteracts the hypoxia-induced inhibition of spontaneously firing hippocampal neurons: a microelectrode array study. PLoS One. 7:e41530.
Goussakov I, Miller MB, Stutzmann GE. 2010. NMDA-mediated Ca(2+) influx drives aberrant ryanodine receptor activation in dendrites of young Alzheimer's disease mice. J Neurosci. 30:12128–12137.
Hsiao K, Chapman P, Nilsen S, Eckman C, Harigaya Y, Younkin S, Yang F, Cole G. 1996. Correlative memory deficits, Abeta elevation, and amyloid plaques in transgenic mice. Science. 274:99–102.
Hu H, Shao LR, Chavoshy S, Gu N, Trieb M, Behrens R, Laake P, Pongs O, Knaus HG, Ottersen OP, et al. 2001. Presynaptic Ca2+-activated K+ channels in glutamatergic hippocampal terminals and their role in spike repolarization and regulation of transmitter release. J Neurosci. 21:9585–9597.
Kuperstein I, Broersen K, Benilova I, Rozenski J, Jonckheere W, Debulpaep M, Vandersteen A, Segers-Nolten I, Van Der Werf K, Subramaniam V, et al. 2010. Neurotoxicity of Alzheimer's disease Abeta peptides is induced by small changes in the Abeta42 to Abeta40 ratio. EMBO J. 29:3408–3420.
LaFerla FM. 2002. Calcium dyshomeostasis and intracellular signalling in Alzheimer's disease. Nat Rev Neurosci. 3:862–872.
Lambert MP, Barlow AK, Chromy BA, Edwards C, Freed R, Liosatos M, Morgan TE, Rozovsky I, Trommer B, Viola KL, et al. 1998. Diffusible, nonfibrillar ligands derived from Abeta1-42 are potent central nervous system neurotoxins. Proc Natl Acad Sci USA. 95:6448–6453.
Lazzari C, Kipanyula MJ, Agostini M, Pozzan T, Fasolato C. 2014. Abeta42 oligomers selectively disrupt neuronal calcium release. Neurobiol Aging. 36:877–885.
Lee L, Kosuri P, Arancio O. 2013. Picomolar amyloid-beta peptides enhance spontaneous astrocyte calcium transients. J Alzheimers Dis. 38:49–62.
Malenka RC, Kauer JA, Zucker RS, Nicoll RA. 1988. Postsynaptic calcium is sufficient for potentiation of hippocampal synaptic transmission. Science. 242:81–84.
Manassero G, Guglielmotto M, Zamfir R, Borghi R, Colombo L, Salmona M, Perry G, Odetti P, Arancio O, Tamagno E, et al. 2016. Beta-amyloid 1-42 monomers, but not oligomers, produce PHF-like conformation of Tau protein. Aging Cell. 15:914–923.
Marcantoni A, Carabelli V, Vandael DH, Comunanza V, Carbone E. 2009. PDE type-4 inhibition increases L-type Ca(2+) currents, action potential firing, and quantal size of exocytosis in mouse chromaffin cells. Pflugers Arch. 457:1093–1110.
Marcantoni A, Raymond EF, Carbone E, Marie H. 2014. Firing properties of entorhinal cortex neurons and early alterations in an Alzheimer's disease transgenic model. Pflugers Arch. 466:1437–1450.
Marcantoni A, Vandael DH, Mahapatra S, Carabelli V, Sinnegger-Brauns MJ, Striessnig J, Carbone E. 2010. Loss of Cav1.3 channels reveals the critical role of L-type and BK channel coupling in pacemaking mouse adrenal chromaffin cells. J Neurosci. 30:491–504.
Marchetti C, Marie H. 2011. Hippocampal synaptic plasticity in Alzheimer's disease: what have we learned so far from transgenic models? Rev Neurosci. 22:373–402.
Marrion NV, Tavalin SJ. 1998. Selective activation of Ca2+-activated K+ channels by co-localized Ca2+ channels in hippocampal neurons. Nature. 395:900–905.
Martire M, Barrese V, D'Amico M, Iannotti FA, Pizzarelli R, Samengo I, Viggiano D, Ruth P, Cherubini E, Taglialatela M. 2010. Pre-synaptic BK channels selectively control glutamate versus GABA release from cortical and hippocampal nerve terminals. J Neurochem. 115:411–422.
Mattson, MP. 2010. ER calcium and Alzheimer's disease: in a state of flux. Sci Signal. 3:pe10.
Minkeviciene R, Rheims S, Dobszay MB, Zilberter M, Hartikainen J, Fulop L, Penke B, Zilberter Y, Harkany T, Pitkanen A, et al. 2009. Amyloid beta-induced neuronal hyperexcitability triggers progressive epilepsy. J Neurosci. 29:3453–3462.
Mucke L, Selkoe DJ. 2012. Neurotoxicity of amyloid beta-protein: synaptic and network dysfunction. Cold Spring Harb Perspect Med. 2:a006338.
Murphy TH, Blatter LA, Wier WG, Baraban JM. 1992. Spontaneous synchronous synaptic calcium transients in cultured cortical neurons. J Neurosci. 12:4834–4845.
Oules B, Del Prete D, Greco B, Zhang X, Lauritzen I, Sevalle J, Moreno S, Paterlini-Brechot P, Trebak M, Checler F, et al. 2012. Ryanodine receptor blockade reduces amyloid-beta load and memory impairments in Tg2576 mouse model of Alzheimer disease. J Neurosci. 32:11820–11834.
Palop JJ, Mucke L. 2010. Amyloid-beta-induced neuronal dysfunction in Alzheimer's disease: from synapses toward neural networks. Nat Neurosci. 13:812–818.
Puzzo D, Gulisano W, Arancio O, Palmeri A. 2015. The keystone of Alzheimer pathogenesis might be sought in Abeta physiology. Neuroscience. 307:26–36.
Puzzo D, Privitera L, Leznik E, Fa M, Staniszewski A, Palmeri A, Arancio O. 2009. Picomolar amyloid-beta positively modulates synaptic plasticity and memory in hippocampus. J Neurosci. 28:14537–14545.
Raffaelli G, Saviane C, Mohajerani MH, Pedarzani P, Cherubini E. 2004. BK potassium channels control transmitter release at CA3-CA3 synapses in the rat hippocampus. J Physiol. 557:147–157.
Ripoli C, Piacentini R, Riccardi E, Leone L, Li Puma DD, Bitan G, Grassi C. 2013. Effects of different amyloid beta-protein analogues on synaptic function. Neurobiol Aging. 34:1032–1044.
Riquelme D, Alvarez A, Leal N, Adasme T, Espinoza I, Valdes JA, Troncoso N, Hartel S, Hidalgo J, Hidalgo C, et al. 2010. High-frequency field stimulation of primary neurons enhances ryanodine receptor-mediated Ca2+ release and generates hydrogen peroxide, which jointly stimulate NF-kappaB activity. Antioxid Redox Signal. 14:1245–1259.
Stocker M, Krause M, Pedarzani P. 1999. An apamin-sensitive Ca2+-activated K+ current in hippocampal pyramidal neurons. Proc Natl Acad Sci USA. 96:4662–4667.

Storm JF. 1987. Action potential repolarization and a fast after-hyperpolarization in rat hippocampal pyramidal cells. J Physiol. 385:733–759.

Stutzmann GE, Caccamo A, LaFerla FM, Parker I. 2004. Dysregulated IP3 signaling in cortical neurons of knock-in mice expressing an Alzheimer's-linked mutation in presenilin1 results in exaggerated Ca2+ signals and altered membrane excitability. J Neurosci. 24:508–513.

Supnet C, Grant J, Kong H, Westaway D, Mayne M. 2006. Amyloid-beta-(1-42) increases ryanodine receptor-3 expression and function in neurons of TgCRND8 mice. J Biol Chem. 281:38440–38447.

Tamagnini F, Scullion S, Brown JT, Randall AD. 2015. Intrinsic excitability changes induced by acute treatment of hippocampal CA1 pyramidal neurons with exogenous amyloid beta peptide. Hippocampus. 25:786–797.

Tamagno E, Bardini P, Guglielmotto M, Danni O, Tabaton M. 2006. The various aggregation states of beta-amyloid 1-42 mediate different effects on oxidative stress, neurodegeneration, and BACE-1 expression. Free Radic Biol Med. 41: 202–212.

Thibault O, Gant JC, Landfield PW. 2007. Expansion of the calcium hypothesis of brain aging and Alzheimer's disease: minding the store. Aging Cell. 6:307–317.

Thibault O, Pancani T, Landfield PW, Norris CM. 2012. Reduction in neuronal L-type calcium channel activity in a double knock-in mouse model of Alzheimer's disease. Biochim Biophys Acta. 1822:546–549.

van den Pol AN, Finkbeiner SM, Cornell-Bell AH. 1992. Calcium excitability and oscillations in suprachiasmatic nucleus neurons and glia in vitro. J Neurosci. 12:2648–2664.

Vandael DH, Marcantoni A, Carbone E. 2015. Cav1.3 Channels as Key Regulators of Neuron-Like Firings and Catecholamine Release in Chromaffin Cells. Curr Mol Pharmacol. 8:149–161.

Vandael DH, Marcantoni A, Mahapatra S, Caro A, Ruth P, Zuccotti A, Knipper M, Carbone E. 2010. Ca(v)1.3 and BK channels for timing and regulating cell firing. Mol Neurobiol. 42:185–198.

Vandael DH, Zuccotti A, Striessnig J, Carbone E. 2012. Ca(V)1.3-driven SK channel activation regulates pacemaking and spike frequency adaptation in mouse chromaffin cells. J Neurosci. 32:16345–16359.

Wang S, Polo-Parada L, Landmesser LT. 2009. Characterization of rhythmic Ca2+ transients in early embryonic chick motoneurons: Ca2+ sources and effects of altered activation of transmitter receptors. J Neurosci. 29:15232–15244.

Wang Y, Mattson MP. 2013. L-type Ca2+ currents at CA1 synapses, but not CA3 or dentate granule neuron synapses, are increased in 3xTgAD mice in an age-dependent manner. Neurobiol Aging. 35:88–95.

Westenbroek RE, Ahlijanian MK, Catterall WA. 1990. Clustering of L-type Ca2+ channels at the base of major dendrites in hippocampal pyramidal neurons. Nature. 347:281–284.

Ye H, Jalini S, Mylvaganam S, Carlen P. 2010. Activation of large-conductance Ca(2+)-activated K(+) channels depresses basal synaptic transmission in the hippocampal CA1 area in APP (swe/ind) TgCRND8 mice. Neurobiol Aging. 31:591–604.

Yu JT, Chang RC, Tan L. 2009. Calcium dysregulation in Alzheimer's disease: from mechanisms to therapeutic opportunities. Prog Neurobiol. 89:240–255.

Zhou Y, Lingle CJ. 2014. Paxilline inhibits BK channels by an almost exclusively closed-channel block mechanism. J Gen Physiol. 144:415–440.